Smart Mater. Struct. **19** (2010) 115022 (11pp) doi:10.1088/0964-1726/19/11/115022

Nonlinear dynamics and chaos in a pseudoelastic two-bar truss

Marcelo A Savi and Jefferson B Nogueira

COPPE—Department of Mechanical Engineering, Universidade Federal do Rio de Janeiro, 21.941.972, Rio de Janeiro, RJ, PO Box 68.503, Brazil

E-mail: savi@mecanica.ufrj.br

Received 10 March 2010, in final form 26 August 2010
Published 5 October 2010
Online at stacks.iop.org/SMS/19/115022

Abstract
Stability aspects of structures are usually treated by archetypal models that provide global comprehension of the system behavior. The two-bar truss is an example of this kind of model that presents snap-through behavior. This paper deals with the dynamical response of a pseudoelastic two-bar truss, representing an archetypal model of a structural system that exhibits both geometrical and constitutive nonlinearities. Adaptive trusses with shape memory alloy actuators are examples of dynamical systems that may behave like the structure considered in this paper. A constitutive model is employed in order to describe the SMA behavior, presenting close agreement with experimental data. An iterative numerical procedure based on the operator split technique, the orthogonal projection algorithm and the classical fourth order Runge–Kutta method is developed to deal with nonlinearities in the formulation. Numerical investigation is carried out considering free and forced responses of the pseudoelastic two-bar truss showing complex behaviors.

1. Introduction

The stability analysis of structural systems is the objective of many research efforts related to complex behaviors. In this regard, archetypal models are usually employed in order to investigate the general aspects of the structural dynamics, providing global comprehension of the system behavior. An archetypal model used to analyze the stability aspects of structures is the two-bar truss. This kind of system allows one to analyze bifurcation scenarios related to stability changes associated with the different characteristics of buckling behavior. The symmetric two-bar truss, known as the von Mises truss, represents one of the most popular systems related to stability analysis, defining some of the most important characteristics of framed structures and flat arches, and of many other physical phenomena associated with bifurcation buckling (Bazant and Cedolin 1991).

One of the remarkable properties of the von Mises truss is that, for a given load level, two displacement configurations are possible. If the structure is loaded with a monotonically increasing force, the displacement path may jump from one configuration to another, presenting snap-through behavior. Post-buckling aspects of different kinds of structures are usually analyzed by considering snap-through behavior, such as in trusses (Tada and Suito 1998), cylindrical shells (Gonçalves and Del Prado 2002, Soliman and Gonçalves 2003), thin films (Parry *et al* 2005), and laminated composites failures (Choi *et al* 1999). Snap-through behavior is a classical geometrical nonlinearity and, therefore, the nonlinear dynamics of the von Mises truss may exhibit a number of interesting, complex behaviors. This nonlinear dynamics can be properly represented by the two-well potential problem described by the Duffing equation (Ario 2004).

The combination of geometrical and constitutive nonlinearities may further increase the complex nonlinear dynamics of this kind of system. Yankelevsky (1999) introduced elasto-plastic material behavior, showing its influence in the dynamical response of a two-bar truss. Savi *et al* (2002a) analyzed a two-bar truss built with shape memory alloys (SMAs) that presents a very complex behavior.

Shape memory alloys belong to the class of smart materials being used in different kinds of applications (Lagoudas 2008, Paiva and Savi 2006, Machado and Savi 2003). Among different thermomechanical behaviors, SMAs present both pseudoelastic and shape memory effects that are associated with thermoelastic martensitic transformations. The shape memory effect, present in various metallic alloys, is a phenomenon where deformed objects may recover their

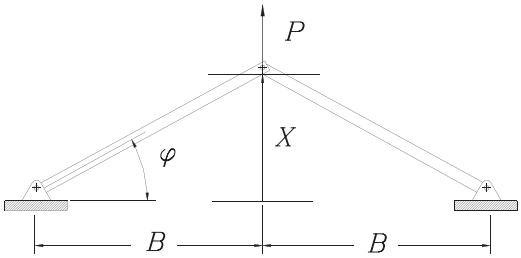

Figure 1. Two-bar truss (von Mises truss).

original form after going through a proper heat treatment. Pseudoelastic behavior, on the other hand, is characterized by complete strain recovery accompanied by a large hysteresis in a loading–unloading cycle (Paiva and Savi 2006). The nonlinear dynamics of SMA oscillators is treated by different references that show a very complex behavior (Savi and Braga 1993a, 1993b, Machado *et al* 2004, Savi and Pacheco 2002, Machado *et al* 2003, Lacarbonara and Vestroni 2003, Lacarbonara *et al* 2004, Bernardini and Rega 2005, Savi *et al* 2006, Santos and Savi 2009, Machado *et al* 2009).

This paper deals with the dynamical response of a pseudoelastic two-bar truss that represents an archetypal model of a structural system exhibiting both geometrical and constitutive nonlinearities. Adaptive trusses with shape memory alloy actuators are examples of dynamical systems that may behave like the structure considered in this paper. Savi *et al* (2002a) treated an SMA two-bar truss system by considering a polynomial constitutive model to describe the thermomechanical behavior of an SMA bar. This simple model can represent some aspects of SMA behavior, but does not properly represent the hysteresis loop. Here, a more sophisticated constitutive model is employed in order to describe the SMA behavior (Paiva *et al* 2005, Savi and Paiva 2005, Monteiro Jr *et al* 2009, Aguiar *et al* 2010, Oliveira *et al* 2010). This constitutive model presents close agreement with experimental data and, therefore, can represent more accurately the qualitative behavior previously analyzed in the cited reference. An iterative numerical procedure based on the operator split technique (Ortiz *et al* 1983), the orthogonal projection algorithm (Savi *et al* 2002b) and the classical fourth order Runge–Kutta method is developed to deal with nonlinearities in the formulation. Numerical investigation is carried out by considering the free and forced responses of the pseudoelastic two-bar truss, showing a number of interesting, complex behaviors.

2. Equations of motion

Archetypal models are usually employed in order to investigate the general aspects of complex system dynamics, providing global comprehension of the system behavior. The analysis of adaptive trusses with shape memory alloy actuators may be investigated by an archetypal model composed of a plane two-bar truss formed by two identical bars that present only vertical, symmetrical motions. The thermomechanical behavior of the SMA is described by assuming a homogeneous phase

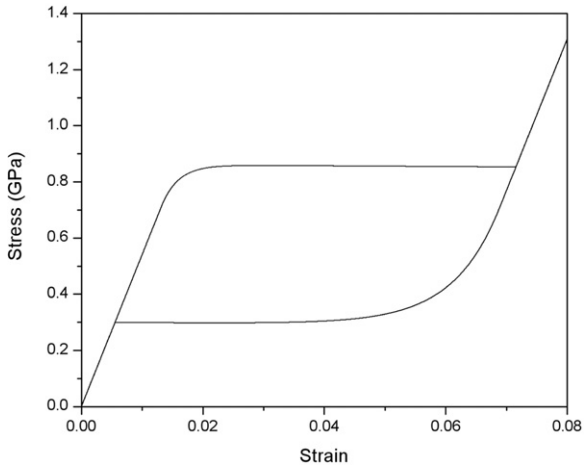

Figure 2. Stress–strain curve ($T = 373$ K).

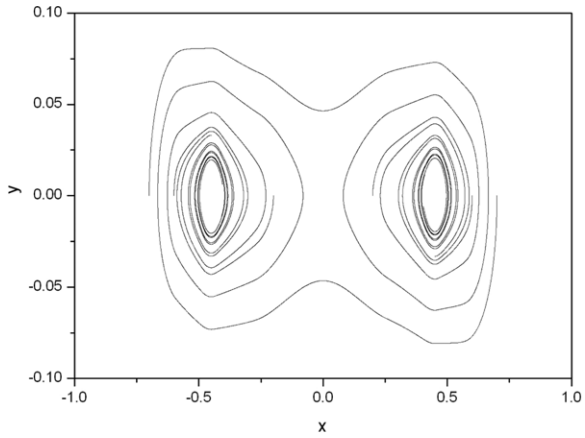

Figure 3. High temperature free vibration.

transformation through the truss. Therefore, constitutive modeling assumes a single-point description and the resulting discrete dynamical system is essentially one-dimensional.

As depicted in figure 1, the two-bar truss is a plane, framed structure, formed by two identical bars, both making an angle φ with an horizontal line, and free to rotate around their supports and at the joint. The structure's mass is assumed to be lumped at the node, and only vertical, symmetrical motions of the truss are considered. Under these assumptions, the structure is divided into segments without mass, connected by nodes with lumped mass, m. In the present investigation we consider a pseudoelastic two-bar truss. The two identical bars are built with shape memory alloys having length l and cross section area A. The critical Euler load of each bar is assumed to be sufficiently large so that buckling will not occur in the simulations reported here.

The symmetric, vertical displacement is denoted by X. Moreover, it is assumed that there is a linear viscous damping represented by a coefficient c. Therefore, the balance of momentum is expressed through the following equation of motion,

$$-2F\sin\varphi - c\dot{X} + P = m\ddot{X} \tag{1}$$

where F is the force on each bar and P is an external force.

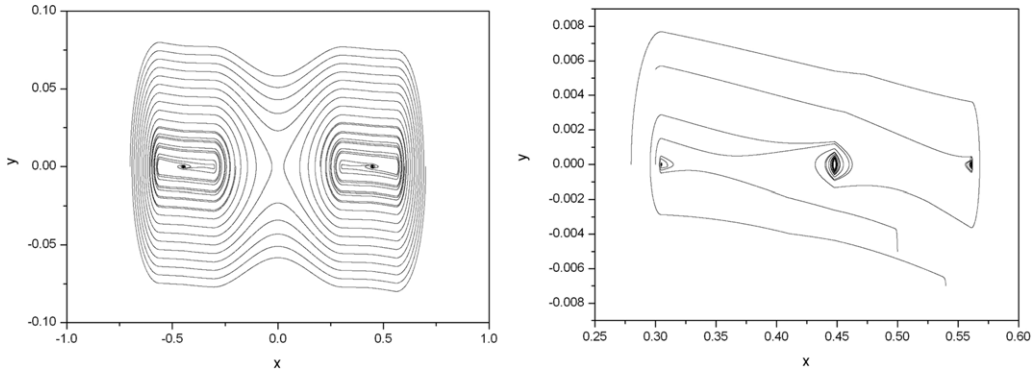

Figure 4. Low temperature free vibration.

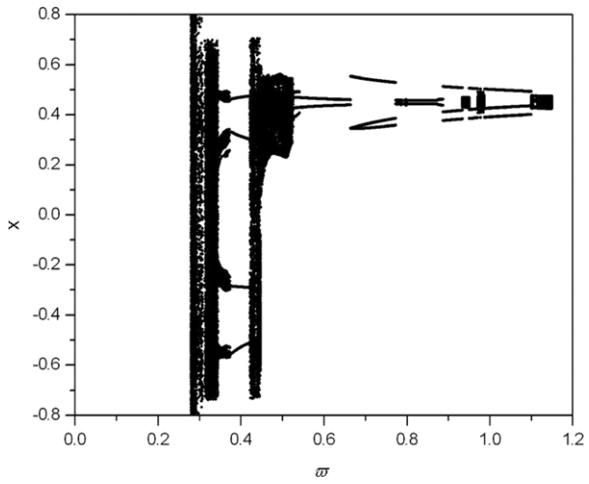

Figure 5. Bifurcation diagram varying ϖ with $\gamma = 0.01$.

The description of force F is related to the SMA thermomechanical behavior and it is assumed that phase transformations are homogeneous throughout the truss. There are different ways to describe the SMA behavior and, here, a constitutive model with internal variables previously discussed in different references (Savi *et al* 2002b, Baêta-Neves *et al* 2004, Paiva *et al* 2005, Savi and Paiva 2005, Monteiro Jr *et al* 2009, Aguiar *et al* 2010, Oliveira *et al* 2010) is employed.

In order to present the constitutive equations, let us consider strain (ε), temperature (T), and three more state variables associated with the volume fraction of each macroscopic phase: β_1 is associated with tensile detwinned martensite, β_2 is related to compressive detwinned martensite, β_3 represents austenite. Actually, a fourth phase β_4 related to twinned martensite is considered, which can be obtained from the phase coexistence condition ($\beta_4 = 1 - \beta_1 + \beta_2 + \beta_3$). With this assumption, it is possible to obtain a complete set of constitutive equations that describes the thermomechanical behavior of SMAs as follows:

$$\sigma = E\varepsilon + [\alpha + E\alpha_{\mathrm{h}}](\beta_2 - \beta_1) - \Omega(T - T_0) \tag{2}$$

$$\dot{\beta}_1 = \frac{1}{\eta}\{\alpha\varepsilon + \Lambda + [2\alpha_{\mathrm{h}}\alpha + E\alpha_{\mathrm{h}}^2](\beta_2 - \beta_1) + \alpha_{\mathrm{h}}[E\varepsilon - \Omega(T - T_0)] - \partial_1 J_\pi\} + \partial_1 J_\chi \tag{3}$$

$$\dot{\beta}_2 = \frac{1}{\eta}\{-\alpha\varepsilon + \Lambda - [2\alpha_{\mathrm{h}}\alpha + E\alpha_{\mathrm{h}}^2](\beta_2 - \beta_1) - \alpha_{\mathrm{h}}[E\varepsilon - \Omega(T - T_0)] - \partial_2 J_\pi\} + \partial_2 J_\chi \tag{4}$$

$$\dot{\beta}_3 = \frac{1}{\eta}\left\{-\frac{1}{2}(E_{\mathrm{A}} - E_{\mathrm{M}})[\varepsilon + \alpha_{\mathrm{h}}(\beta_2 - \beta_1)]^2 + \Lambda_3 + (\Omega_{\mathrm{A}} - \Omega_{\mathrm{M}})(T - T_0)[\varepsilon + \alpha_{\mathrm{h}}(\beta_2 - \beta_1)] - \partial_3 J_\pi\right\} + \partial_3 J_\chi \tag{5}$$

where $E = E_{\mathrm{M}} + \beta_3(E_{\mathrm{A}} - E_{\mathrm{M}})$ is the elastic modulus while $\Omega = \Omega_{\mathrm{M}} + \beta_3(\Omega_{\mathrm{A}} - \Omega_{\mathrm{M}})$ is related to the thermal expansion coefficient. Note that subscript 'A' refers to the austenitic phase, while 'M' refers to martensite. Moreover, parameters $\Lambda = \Lambda(T)$ and $\Lambda_3 = \Lambda_3(T)$ are associated with phase transformation stress levels. Parameter α_{h} is introduced in order to define the horizontal width of the stress–strain hysteresis loop, while α helps vertical hysteresis loop control on the stress–strain diagrams.

The terms $\partial_n J_\pi$ ($n = 1, 2, 3$) are sub-differentials of the indicator function J_π with respect to β_n (Rockafellar 1970). The indicator function $J_\pi = J_\pi(\beta_1, \beta_2, \beta_3)$ is related to a convex set π, which provides the internal constraints related to the phases' coexistence. With respect to evolution equations of volume fractions, η_1, η_2 and η_3 represent the internal dissipation related to phase transformations. Moreover $\partial_n J_\chi$ ($n = 1, 2, 3$) are sub-differentials of the indicator function J_χ with respect to $\dot{\beta}_n$ (Rockafellar 1970). This indicator function is associated with the convex set χ, which establishes conditions for the correct description of internal subloops due to incomplete phase transformations and also avoids phase transformations $M+ \rightarrow M$ or $M- \rightarrow M$.

Regarding the parameter definitions, temperature dependent relations are adopted for Λ and Λ_3 as follows:

$$\Lambda = \begin{cases} -L_0 + \dfrac{L}{T_{\mathrm{M}}}(T - T_{\mathrm{M}}) & \text{if } T > T_{\mathrm{M}} \\ -L_0 & \text{if } T \leqslant T_{\mathrm{M}} \end{cases} \tag{6a}$$

$$\Lambda_3 = \begin{cases} -L_0^{\mathrm{A}} + \dfrac{L^{\mathrm{A}}}{T_{\mathrm{M}}}(T - T_{\mathrm{M}}) & \text{if } T > T_{\mathrm{M}} \\ -L_0^{\mathrm{A}} & \text{if } T \leqslant T_{\mathrm{M}}. \end{cases} \tag{6b}$$

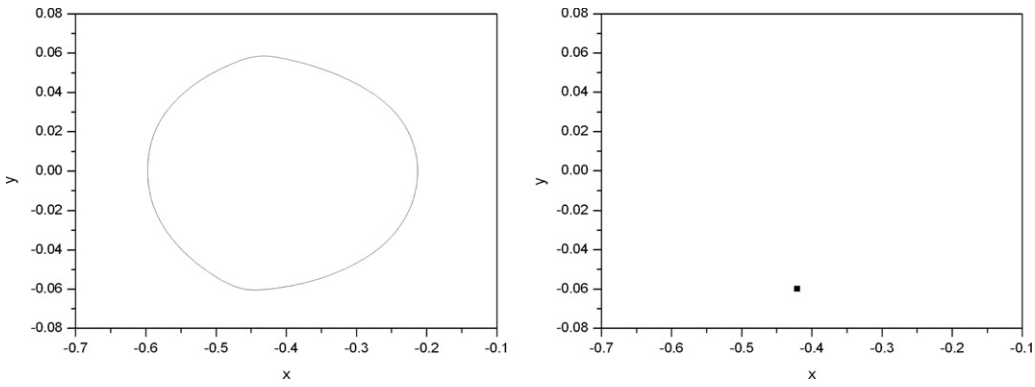

Figure 6. Period-1 response for $\gamma = 0.01$ and $\varpi = 0.3$, oscillating around the truss lower position.

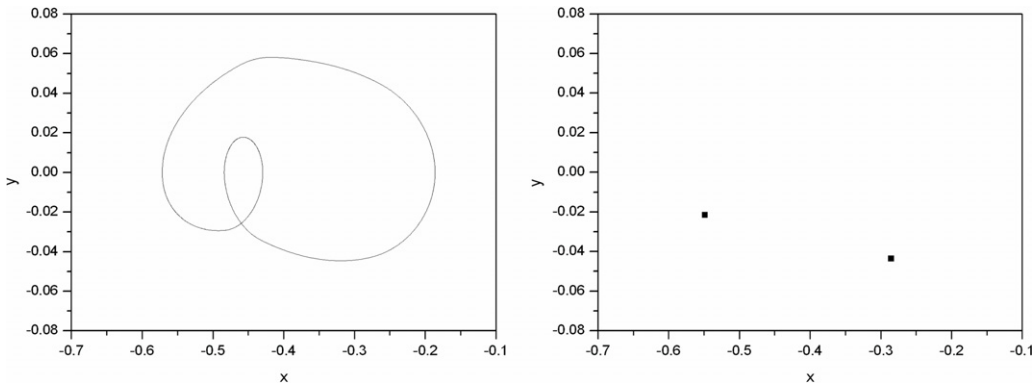

Figure 7. Period-2 response for $\gamma = 0.01$ and $\varpi = 0.382$, oscillating around the truss lower position.

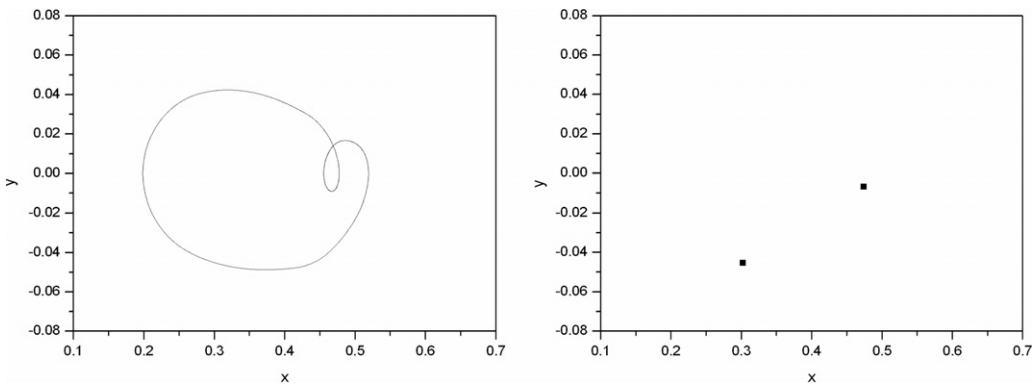

Figure 8. Period-2 response for $\gamma = 0.01$ and $\varpi = 0.42$, oscillating around the truss upper position.

Here, T_M is the temperature below which the martensitic phase becomes stable in a stress-free state. Besides, L_0, L, L_0^A and L^A are parameters related to the critical stress for phase transformation.

In order to study the different characteristics of the kinetics of phase transformation for the loading and unloading processes, it is possible to consider different values for the internal dissipation parameter η_n ($n = 1, 2, 3$): η_n^L and η_n^U during the loading and unloading processes, respectively. For more details about the constitutive model, see Paiva *et al* (2005) and Savi and Paiva (2005).

At this point, it is necessary to define the two-bar truss strain in order to allow the use of the constitutive equation in the equilibrium equation (1). Hence, by assuming the strain as follows:

$$\varepsilon = \frac{L}{L_0} - 1 = \frac{\cos\varphi_0}{\cos\varphi} - 1 \tag{7}$$

the equation of motion may be rewritten:

$$m\ddot{X} + c\dot{X} + 2A\frac{X}{(X^2+B^2)^{1/2}}\left\{E\left[\frac{(X^2+B^2)^{1/2}}{L_0} - 1\right] + [\alpha + E\alpha_h](\beta_2 - \beta_1) - \Omega(T - T_0)\right\} = P(t) \tag{8}$$

where B is the horizontal projection of each truss bar (figure 1).

Considering a periodic excitation $P = P_0\sin(\omega t)$, the equation of motion may be written in non-dimensional form

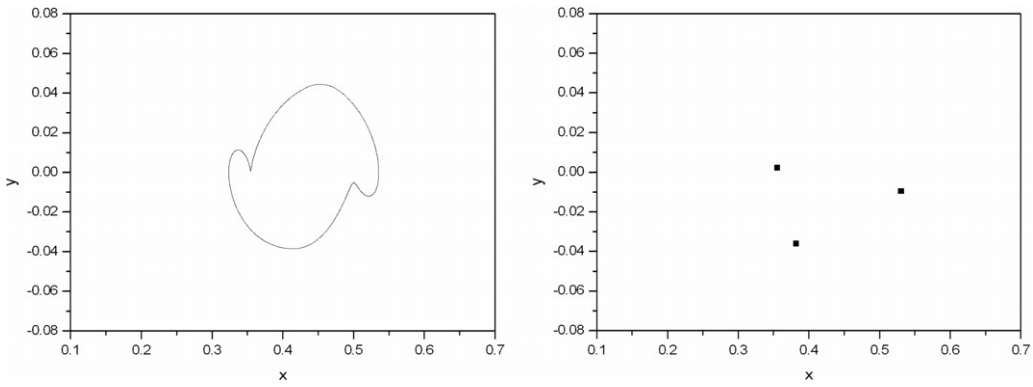

Figure 9. Period-3 response for $\gamma = 0.01$ and $\varpi = 0.76$, oscillating around the truss upper position.

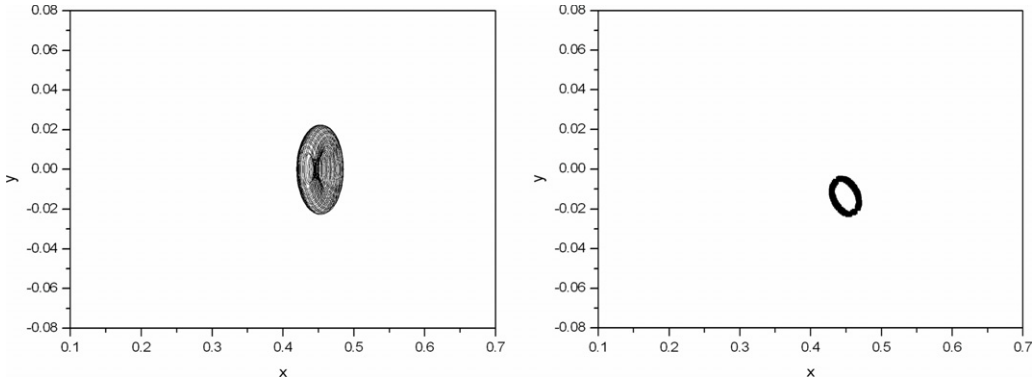

Figure 10. Quasi-periodic response for $\gamma = 0.01$ and $\varpi = 0.9418$.

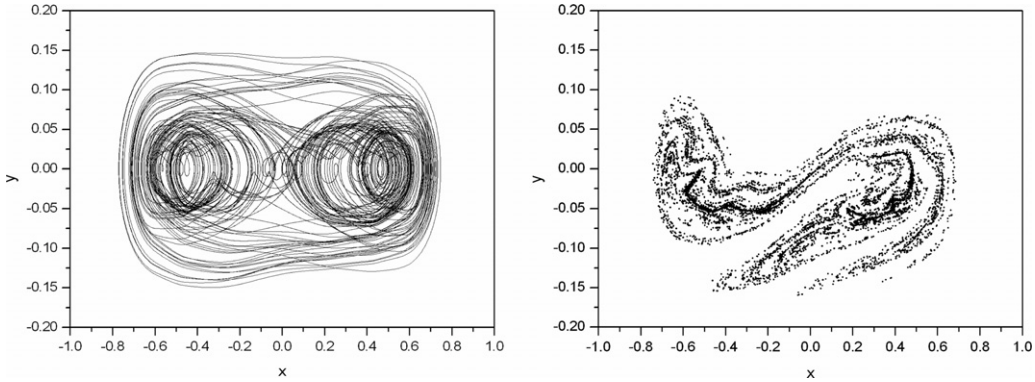

Figure 11. Chaotic-like response for $\gamma = 0.01$ and $\varpi = 0.3347$.

as:

$$x' = y$$

$$y' = \gamma \sin(\varpi\tau) - \xi\, y - \mu_E\left[1 - \frac{1}{(x^2+b^2)^{1/2}}\right]x - [(\hat{\alpha} + \mu_E\alpha_h)(\beta_2 - \beta_1) - \hat{\Omega}\mu_\Omega(\theta - \theta_0)]\frac{x}{(x^2+b^2)^{1/2}} \tag{9}$$

where

$$x = \frac{X}{L}, \qquad b = \frac{B}{L_0}, \qquad \omega_0^2 = \frac{2E_R A}{mL_0},$$
$$\gamma = \frac{P_0}{mL_0\omega_0^2}, \qquad \xi = \frac{c}{m\omega_0}, \qquad \tau = \omega_0 t,$$
$$\varpi = \frac{\omega}{\omega_0}, \qquad \theta = \frac{T}{T_M}, \qquad \mu_E = \frac{E}{E_M},$$
$$\mu_\Omega = \frac{\Omega}{\Omega_R}, \qquad \hat{\alpha} = \frac{\alpha}{E_R}, \qquad \hat{\Omega} = \frac{\Omega_R T_R}{E_R}$$
$$\text{and} \qquad ()' = \frac{\mathrm{d}()}{\mathrm{d}\tau}.$$

Numerical simulations are performed employing the fourth order Runge–Kutta scheme with time steps chosen to be less than $\Delta\tau = \pi/400\varpi$. In all simulations, we have used the material properties presented in table 1. These values were chosen in order to represent a typical SMA behavior as shown

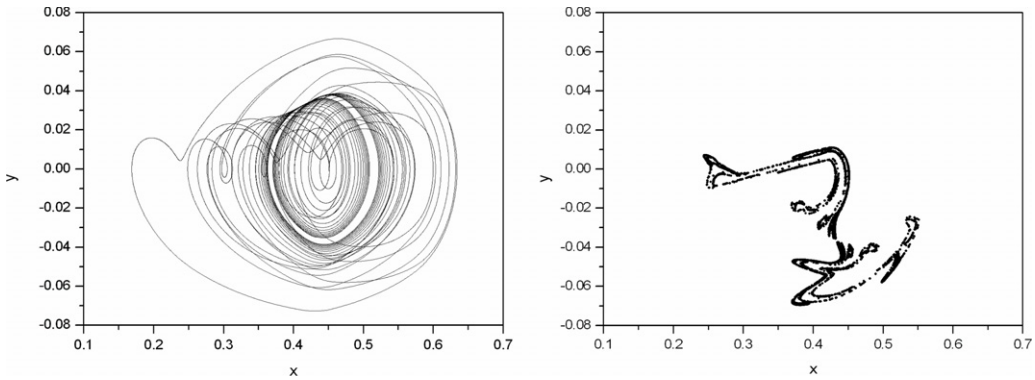

Figure 12. Chaotic-like response for $\gamma = 0.01$ and $\varpi = 0.475$ visiting the truss upper position.

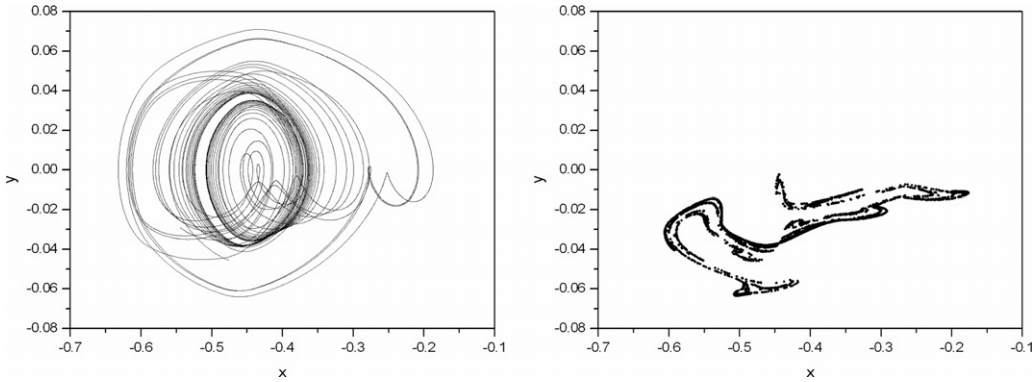

Figure 13. Chaotic-like response for $\gamma = 0.01$ and $\varpi = 0.475$ visiting the truss lower position.

Table 1. SMA constitutive parameters.

E_A (GPa)	E_M (GPa)	α (MPa)	α_h
54	54	150	0.052
L_0 (MPa)	L (MPa)	L_0^A (MPa)	L^A (MPa)
0.15	41.5	0.63	185
Ω_A (MPa K^{-1})	Ω_M (MPa K^{-1})	T_M (K)	T_A (K)
0.74	0.17	291.4	307.7
	η^L (MPa s)	η^U (MPa s)	
	10	27	

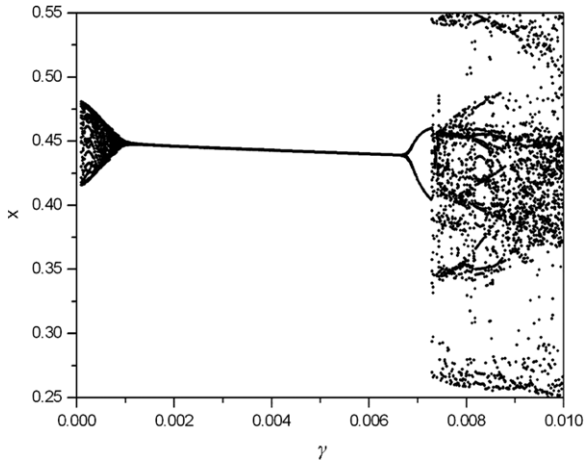

Figure 14. Bifurcation diagram varying forcing amplitude γ for $\varpi = 0.475$.

in figure 2, obtained for a strain driving quasi-static simulation at $T = 373$ K. For the data in table 1, the parameters defined in equation (9) assume the values: $x = 0.447$, $b = 0.894$, $\omega_0^2 = 1.2 \times 10^{10}$, $\xi = 0$, $\theta = 1.28$, $\hat{\alpha} = 2.78 \times 10^{-3}$, $\hat{\Omega} = 5.11 \times 10^{-3}$. We further let $b = 0.866$, corresponding to a two-bar truss with an initial position $\varphi_0 = 30°$.

3. Free vibration

The free response of the SMA two-bar truss is discussed in this section. This is done by letting γ vanish in the equations of motion (9). It is well known that the von Mises truss presents three equilibrium points due to geometrical nonlinearity. Of those, two are stable while the other one is unstable (Bazant and Cedolin 1991). In the case of an SMA two-bar truss, constitutive nonlinearity introduces a different behavior. Savi *et al* (2002a) showed how constitutive nonlinearity represented by the polynomial model changes the structure of the equilibrium points. Nevertheless, since the constitutive model employed in this contribution is more accurate, the original structure of the two-bar truss related to the geometrical nonlinearity has even more changes.

For high temperatures, where only the austenitic phase is present for a stress-free state ($\theta \geqslant \theta_A$), the system has

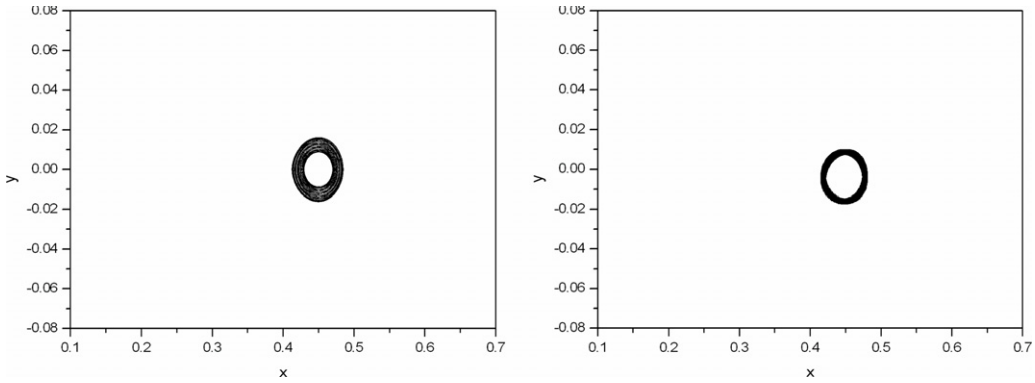

Figure 15. Quasi-periodic response for $\gamma = 2.3 \times 10^{-4}$ and $\varpi = 0.475$.

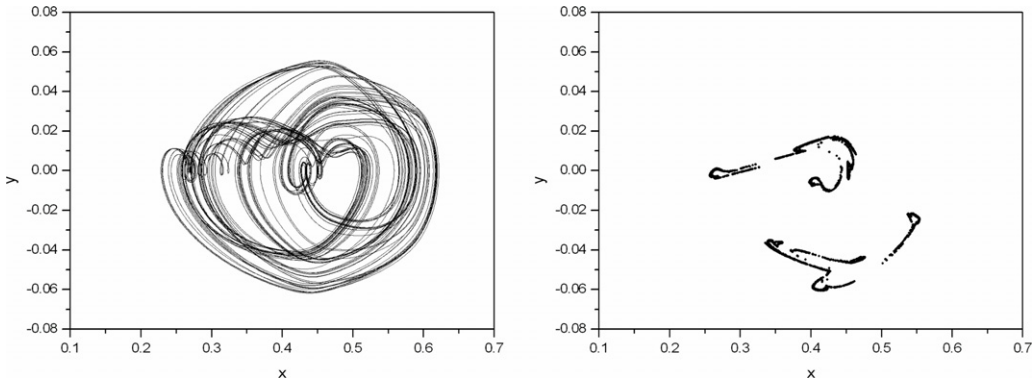

Figure 16. Chaotic-like response for $\gamma = 0.008$ and $\varpi = 0.475$.

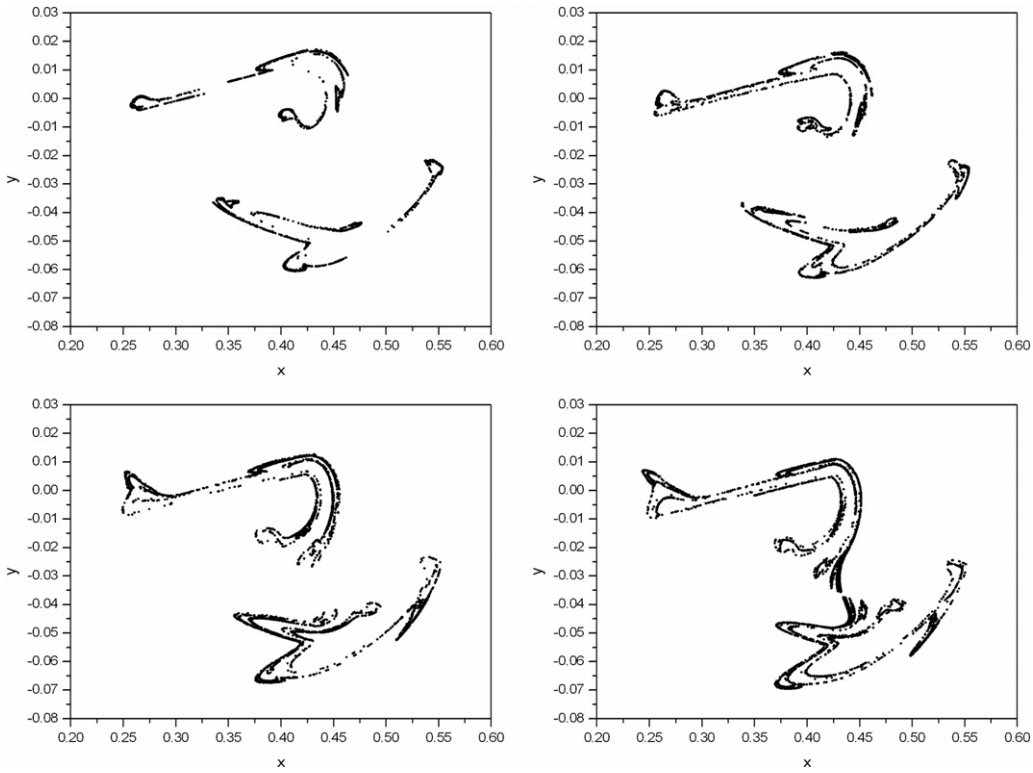

Figure 17. Sequence of four chaotic strange attractors for $\varpi = 0.475$ and different forcing amplitudes $\gamma = 0.0080$, $\gamma = 0.0085$, $\gamma = 0.0095$, $\gamma = 0.0100$, respectively.

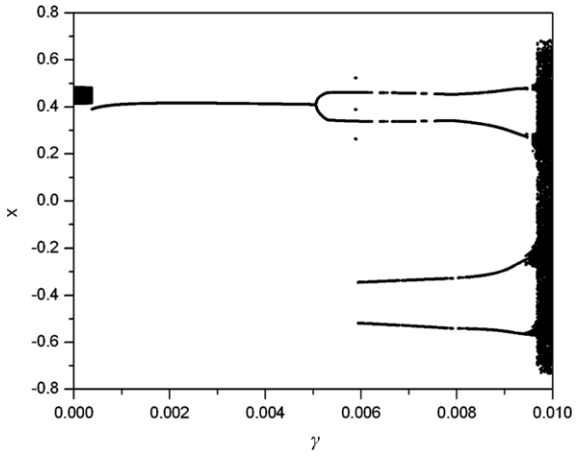

Figure 18. Bifurcation diagram varying the forcing amplitude γ for $\varpi = 0.3347$.

one unstable and two stable equilibrium points. This situation is similar to the geometrical nonlinear system in terms of the number of equilibrium points, however, it should be highlighted that the SMA system tends to dissipate energy due to the hysteresis loop. At low temperatures, where the martensitic phase is stable ($0 < \theta < 1$), constitutive nonlinearity induces the formation of five equilibrium points in the upper position, and another five in the lower position. From each of those sets, three are stable while the others are unstable. These characteristics are related to the stability of martensitic variants.

In order to illustrate the free response of the SMA two-bar truss, we consider a system with $\xi = 0$ in equations (9). Results from simulations are presented in the form of phase portraits. Figure 3 presents the free response of a pseudoelastic system, at higher temperatures, where the austenitic phase is stable in the stress-free state ($\theta = 1.28$). There are, in this case, three equilibrium points. From those, two are stable while the other is unstable. Notice that although the system has no viscous damping, hysteretic behavior dissipates energy until the elastic response is reached in the steady-state. On the other hand, at a lower temperature, where the martensitic phase is present in the alloy, the system has eleven equilibrium points, where six are stable and five are unstable. Figure 4 is representative of the free response at lower temperatures ($\theta = 0.99$) when the alloy is fully martensitic. The right hand side of the picture shows the enlargement of the phase portrait presenting initial conditions that tend to the two-bar truss upper position.

4. Forced vibration

In this section, the forced vibration response is addressed. This analysis is done by considering the high temperature behavior that is related to the pseudoelastic effect where the austenitic phase is stable in the stress-free state.

In order to start the analysis, let us consider the bifurcation diagram which represents stroboscopically sampled displacement values, x, under the slow quasi-static increase of a system parameter. First, the driving frequency, ϖ, is considered, assuming a fixed forcing amplitude $\gamma = 0.01$. Figure 5 presents this bifurcation diagram, showing regions related to a cloud of points and also regions represented by a discrete number of points associated with periodic motions. The differences are noticeable between different frequency values.

Different frequency values are now investigated in order to analyze the system response. Phase space plots and Poincaré sections are presented for each set of parameters. For this forcing amplitude value, when frequency is $\varpi = 0.3$, the system presents a period-1 motion, oscillating around the truss lower position equilibrium point. Note that figure 6 presents a closed curve in phase space and a single point in the Poincaré section. On increasing the frequency to $\varpi = 0.382$, a period-2 motion occurs, once again around the truss lower position (figure 7). Now, the Poincaré section presents two points. When $\varpi = 0.42$, the system still presents a period-2 motion, however, at a different position. Now, the system oscillates around the truss upper position (figure 8). A period-3 motion occurs when $\varpi = 0.76$ (figure 9) and a quasi-periodic motion appears for $\varpi = 0.9418$ (figure 10), presenting a closed curve at the Poincaré section. All these possibilities represent the great complexity related to the SMA two-bar truss dynamical behavior.

Chaotic motion is also a possibility related to the pseudoelastic two-bar truss. On considering $\varpi = 0.3347$, a chaotic-like motion is noticeable, related to a typical strange

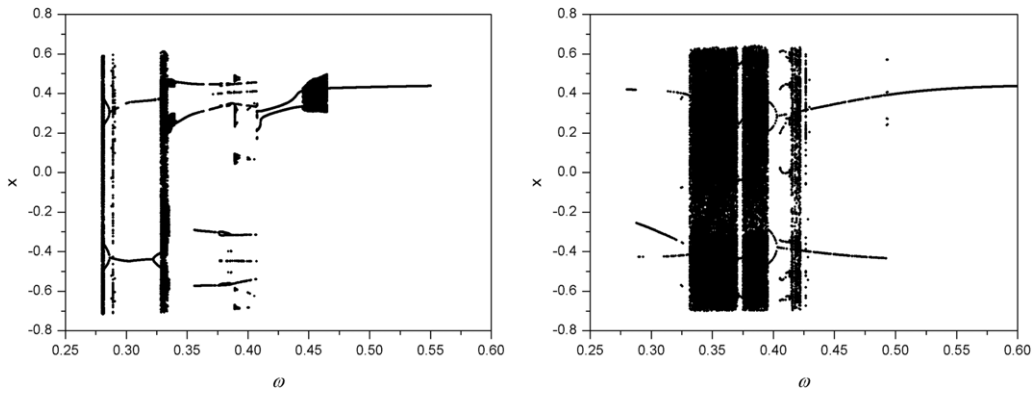

Figure 19. Bifurcation diagrams varying ϖ with $\gamma = 0.01$. SMA truss (left side) and elastic truss (right side).

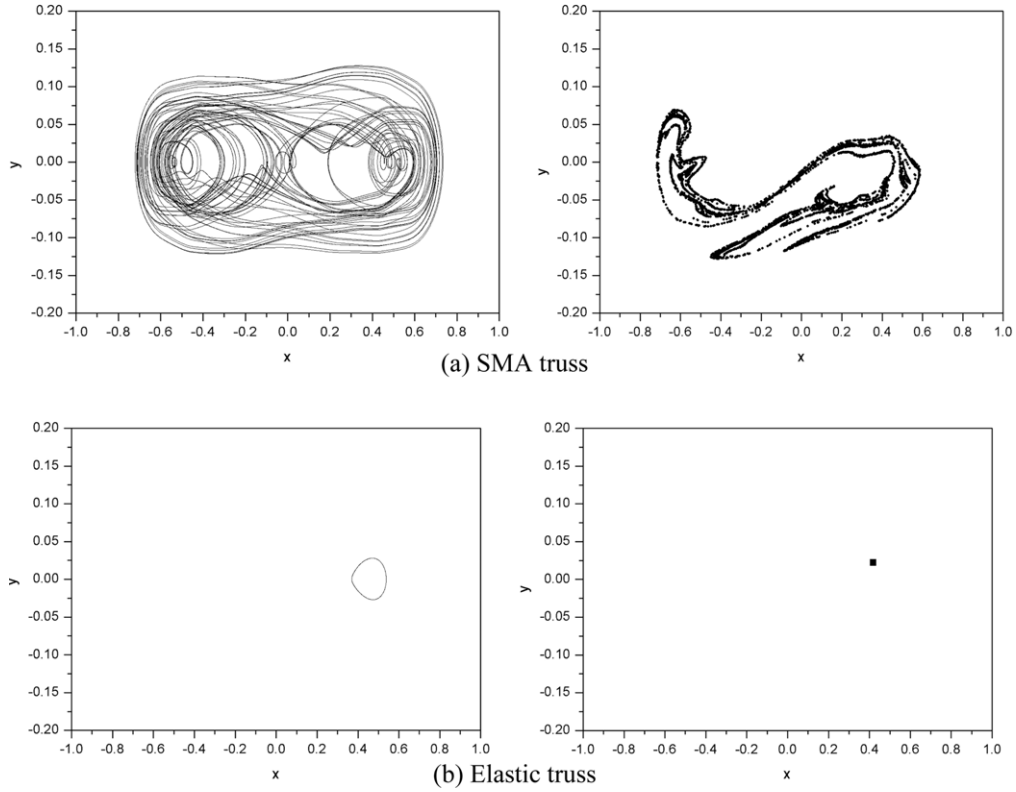

Figure 20. System response for $\xi = 0.02$, $\gamma = 0.01$ and $\varpi = 0.28$. (a) SMA truss: chaotic-like response; (b) elastic truss: period-1 response.

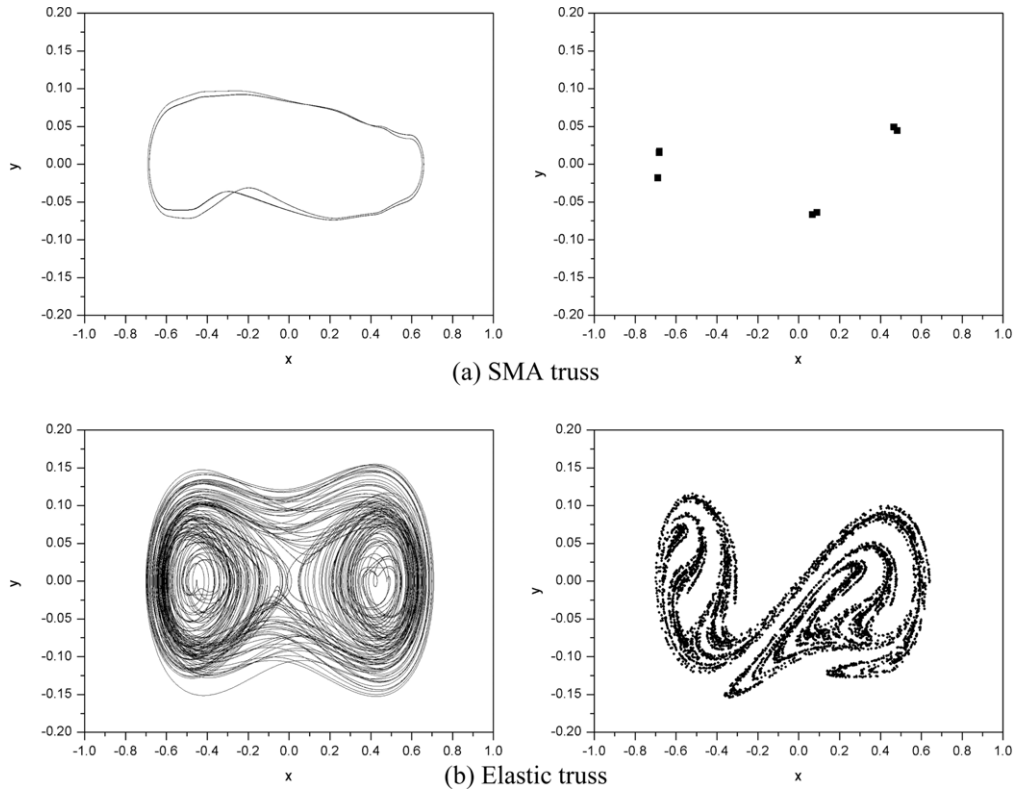

Figure 21. System response for $\xi = 0.02$, $\gamma = 0.01$ and $\varpi = 0.39$. (a) SMA truss: period-6 response; (b) elastic truss: chaotic-like response.

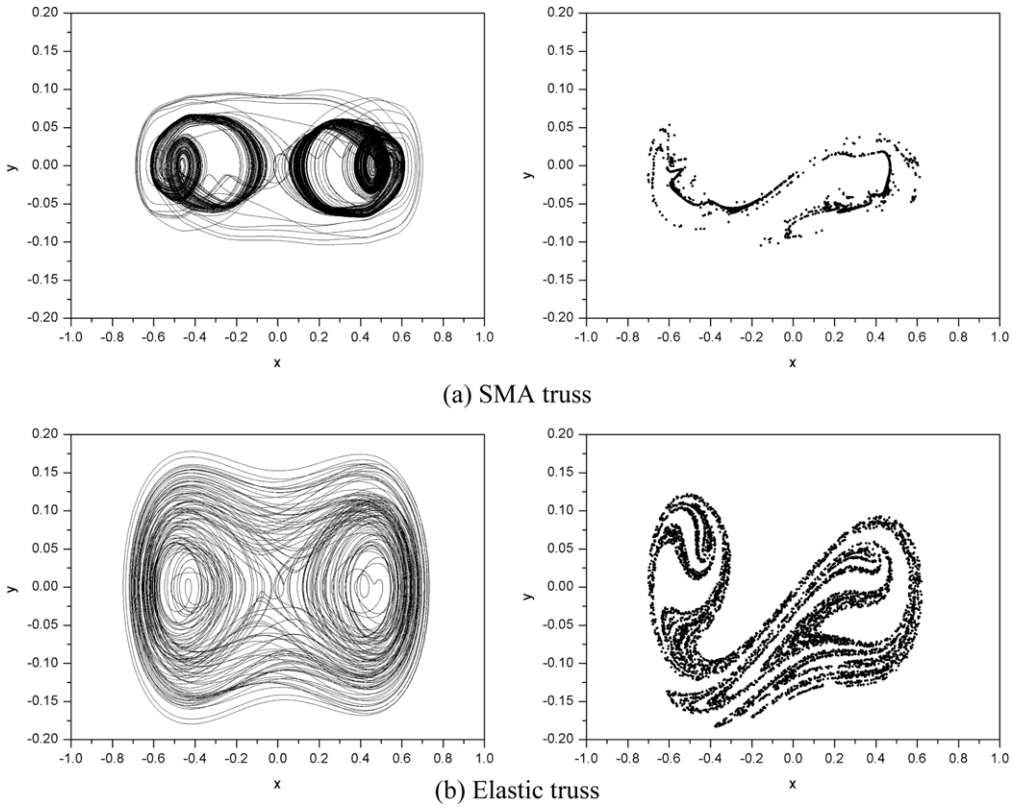

Figure 22. System response for $\xi = 0.02$, $\gamma = 0.01$ and $\varpi = 0.334$. (a) SMA truss: chaotic-like response; (b) elastic truss: chaotic-like response.

attractor observed in the Poincaré section (figure 11). Note that this motion is related to all phase space, visiting all equilibrium points. A different chaotic motion may be induced when $\varpi = 0.475$. Under this condition, the system tends to oscillate only at the truss upper position and the strange attractor is restricted to the positive part of the phase plane (figure 12). The position of the chaotic attractor, however, may be altered by considering appropriate initial conditions, since there is an attractor coexistence. Figure 13 presents the chaotic strange attractor visiting the truss lower position.

The influence of the driving force amplitude is now considered in the bifurcation diagram varying this parameter, assuming a fixed forcing frequency, for example, $\varpi = 0.475$ (figure 14).

Regions at the beginning of the bifurcation diagram are related to quasi-periodic motion, as presented in figure 15. By increasing the forcing parameter, a period-1 motion appears and afterward a period-doubling bifurcation takes place, and the motion tends to become chaotic for values greater than $\gamma = 0.0073$. Figure 16 presents a chaotic-like response for $\gamma = 0.008$, showing a disconnected strange attractor. The increase in the forcing amplitude value tends to form a connected attractor, as can be seen in figure 17, where four forcing amplitudes are considered: $\gamma = 0.0080$, 0.0085, 0.0095 and 0.0100.

At this point, a different frequency value is assumed ($\varpi = 0.3347$) showing how it changes the system response structure. A bifurcation diagram is presented in figure 18 allowing a comparison with figure 14. Basically, quasi-periodic motion is not present in this range of forcing amplitudes and the chaotic region is reduced. The strange attractor type is also modified, and this difference can be observed by comparing figures 11 and 12.

5. SMA and elastic two-bar trusses

Let us now establish a comparison between the dynamical response of an SMA two-bar truss and an elastic truss. Basically, both systems are assumed to have the same stiffness when phase transformations do not take place. We consider a dissipation parameter $\xi = 0.02$ and a force amplitude $\gamma = 0.01$. Bifurcation diagrams for both cases are presented in figure 19, showing the influence of the parameter ϖ. Note that the SMA truss behavior tends to be more regular due the higher dissipation promoted by the hysteresis loop. Moreover, it should be highlighted that both systems can present chaotic and periodic responses under different conditions.

In order to highlight some interesting possibilities, different forcing frequencies are considered. Initially, it is assumed that $\varpi = 0.28$. Under this condition, the SMA truss presents a chaotic-like response and the elastic response has a periodic response (figure 20). By assuming $\varpi = 0.39$, the SMA truss presents a period-6 response while the elastic truss has a chaotic-like response (figure 21). When $\varpi = 0.334$, both trusses present a chaotic-like response (figure 22). This result allows one to compare strange attractor patterns of both responses. Since the SMA system is related to a hysteretic response, its dissipation is considerable greater than the elastic

system and, therefore, an attractor with smaller dimension for the SMA system is expected.

6. Conclusions

This paper reports results from numerical simulations of the dynamical response of a shape memory alloy two-bar truss. This system represents an archetypal model useful for the stability investigation of adaptive trusses with shape memory alloy actuators. A constitutive model with internal constraints is assumed to describe the thermomechanical behavior of the bars. An iterative numerical procedure based on the operator split technique, the orthogonal projection algorithm and the classical fourth order Runge–Kutta method is developed to deal with nonlinearities in the formulation. Numerical investigation is carried out considering free and forced responses of an SMA two-bar truss at high temperatures, presenting pseudoelastic behavior. Free response investigation shows the structure of the equilibrium points and its temperature dependence. It is also clear how the constitutive nonlinearity alters the structure of the equilibrium point when compared to that related to the elastic two-bar truss. Results from forced response analysis show that the system may present a number of interesting, complex behaviors. Periodic, quasi-periodic and chaotic motions are possible in the two-bar truss response. It is also noticeable that the attractor coexistence gives this system a very rich dynamics. Finally, the paper establishes a comparison between a pseudoelastic and an elastic truss, showing the influence of dissipation due to the hysteresis loop.

Acknowledgments

The authors would like to acknowledge the support of the Brazilian Research Agencies CNPq and FAPERJ, the INCT-EIE (National Institute of Science and Technology—Smart Structures in Engineering) and FAPEMIG. The Air Force Office of Scientific Research (AFOSR) is also acknowledged. Finally, it is important to mention the inspirational discussions with James M Fillerup.

References

Aguiar R A A, Savi M A and Pacheco P M C L 2010 Experimental and numerical investigations of shape memory alloy helical springs *Smart Mater. Struct.* **19** 025008

Ario I 2004 Homoclinic bifurcation and chaos attractor in elastic two-bar truss *Int. J. Non-Linear Mech.* **39** 605–17

Baêta-Neves A P, Savi M A and Pacheco P M C L 2004 On the Fremond's constitutive model for shape memory alloys *Mech. Res. Commun.* **31** 677–88

Bazant Z P and Cedolin L 1991 *Stability of Structures* (Oxford: Oxford University Press)

Bernardini D and Rega G 2005 Thermomechanical modelling, nonlinear dynamics and chaos in shape memory oscillators *Math. Comput. Modell. Dyn. Syst.* **11** 291–314

Choi S, Lee J J, Seo D C and Choi S W 1999 The active buckling control of laminated composite beams with embedded shape memory alloy wires *Compos. Struct.* **47** 679–86

Gonçalves P B and Del Prado Z J G N 2002 Nonlinear oscillations and stability of parametrically excited cylindrical shells *Meccanica* **37** 569–97

Lacarbonara W, Bernardini D and Vestroni F 2004 Nonlinear thermomechanical oscillations of shape-memory devices *Int. J. Solids Struct.* **41** 1209–34

Lacarbonara W and Vestroni F 2003 Nonclassical responses of oscillators with hysteresis *Nonlinear Dyn.* **32** 235–58

Lagoudas D C 2008 *Shape Memory Alloys: Modeling and Engineering Applications* (Berlin: Springer)

Machado L G, Lagoudas D C and Savi M A 2009 Lyapunov exponents estimation for hysteretic systems *Int. J. Solids Struct.* **46** 1269–598

Machado L G and Savi M A 2003 Medical applications of shape memory alloys *Braz. J. Med. Biol. Res.* **36** 683–91

Machado L G, Savi M A and Pacheco P M C L 2003 Nonlinear dynamics and chaos in coupled shape memory oscillators *Int. J. Solids Struct.* **40** 5139–56

Machado L G, Savi M A and Pacheco P M C L 2004 Bifurcations and crises in a shape memory oscillator *Shock Vib.* **11** 67–80

Monteiro P C C Jr, Savi M A, Netto T A and Pacheco P M C L 2009 A phenomenological description of the thermomechanical coupling and the rate-dependent behavior of shape memory alloys *J. Intell. Mater. Syst. Struct.* **20** 1675–87

Oliveira S A, Savi M A and Kalamkarov A L 2010 A three-dimensional constitutive model for shape memory alloys *Arch. Appl. Mech.* **80** 1163–75

Ortiz M, Pinsky P M and Taylor R L 1983 Operator split methods for the numerical solution of the elastoplastic dynamic problem *Comput. Methods Appl. Mech. Eng.* **39** 137–57

Paiva A and Savi M A 2006 An overview of constitutive models for shape memory alloys *Math. Problems Eng.* **2006** 56876

Paiva A, Savi M A, Braga A M B and Pacheco P M C L 2005 A constitutive model for shape memory alloys considering tensile-compressive asymmetry and plasticity *Int. J. Solids Struct.* **42** 3439–57

Parry G, Colin J, Coupeau C, Foucher F, Cimetière A and Grilhé J 2005 Snapthrough occurring in the postbuckling of thin films *Appl. Phys. Lett.* **86** 081905

Rockafellar R T 1970 *Convex Analysis* (Princeton, NJ: Princeton University Press)

Santos B C and Savi M A 2009 Nonlinear dynamics of a nonsmooth shape memory alloy oscillator *Chaos Solitons Fractals* **40** 197–209

Savi M A and Braga A M B 1993a Chaotic vibrations of an oscillator with shape memory *J. Braz. Soc. Mech. Sci. Eng.* **15** 1–20

Savi M A and Braga A M B 1993b Chaotic response of a shape memory oscillator with internal constraints *COBEM 93-ABCM: Proc. XII Brazilian Congr. of Mechanical Engineering (Brasília)* pp 33–6

Savi M A and Pacheco P M L C 2002 Chaos and hyperchaos in shape memory systems *Int. J. Bifurcation Chaos* **12** 645–57

Savi M A, Pacheco P M C L and Braga A M B 2002a Chaos in a shape memory two-bar truss *Int. J. Non-linear Mech.* **37** 1387–95

Savi M A and Paiva A 2005 Describing internal subloops due to incomplete phase transformations in shape memory alloys *Arch. Appl. Mech.* **74** 637–47

Savi M A, Paiva A, Baêta-Neves A P and Pacheco P M C L 2002b Phenomenological modeling and numerical simulation of shape memory alloys: a thermo-plastic-phase transformation coupled model *J. Intell. Mater. Syst. Struct.* **13** 261–73

Savi M A, Sa M A N, Paiva A and Pacheco P M C L 2006 Tensile-compressive asymmetry influence on the shape memory alloy system dynamics *Chaos Solitons Fractals* **36** 828–42

Soliman M S and Gonçalves P B 2003 Chaotic behavior resulting in transient and steady state instabilities of pressure-loaded shallow spherical shells *J. Sound Vib.* **259** 497–512

Tada M and Suito A 1998 Static and dynamic post-buckling behavior of truss structures *Eng. Struct.* **20** 384–9

Yankelevsky D Z 1999 Elastic-plastic behavior of a shallow two bar truss *Int. J. Mech. Sci.* **41** 663–75